



Comparative Study of Various Controllers Improved by Swarm Optimization for Nonlinear Active Suspension Systems with Actuator Saturation

Mohammed A. AL-Ali^{1*}**Omar F. Lutfy¹****Huthaifa Al-Khazraj¹**¹*Control and Systems Engineering Department, University of Technology - Iraq, Baghdad 10066, Iraq** Corresponding author's Email: cse.22.19@grad.uotechnology.edu.iq

Abstract: The active suspension systems offer substantial benefits in ride comfort, handling control over traditional passive systems. In this paper, the evaluation of various controllers including the proportional-integral-derivative (PID) controller and the state feedback (SF) controller on the dynamics performance of active suspension systems is presented. Unlike the majority of the previous studies, the nonlinearities and actuator saturation in the mathematical model of the suspension system have been considered for more reasonable representation of the real system. To attain a better performance of the two proposed controllers, a swarm bipolar algorithm (SBA) technique has been introduced to improve the searching process for the optimal values of the controllers' adjustable parameters. The simulation results using MATLAB show that the proposed controllers exhibit a good performance in normal operation and in a robustness test involving system parameters' changes. In terms of improving the response of the system, the SBA-PID controller shows a better response than that of the SBA-SF controller.

Keywords: Active suspension system, Nonlinear control, Actuator saturation, PID controller, State feedback controller, Swarm bipolar algorithm.

1. Introduction

Due to its importance to provide a comfort ride and stability performance with the presence of road disturbance, suspension system is one of the most potential components in the car. The suspension system connects a car to its wheels through a network of springs, shock absorbers, and linkages. A mechanism that physically separates the vehicle's body from its wheels is known as the suspension system. Road comfort is directly improved by the suspension system of the vehicle by minimizing the vertical acceleration transmitted to the passenger [1-3]. Over the past few decades, a significant amount of study has focused on the examination of a variety of suspension system types, such as passive, semiactive, and active suspension systems [4]. In particular, a basic passive suspension system consists of a spring that works as an energy storing element and a damper that works as an energy dissipating element [5]. Unlike the passive suspension system, the semiactive type employs an adjustable damper to

reduce the suspension vibration after the presence of road disturbances [6]. Since the vibration reduction capabilities of previous two types are restricted, the active suspension system has a hydraulic actuator that allows the suspension force to be adjusted based on the vehicle's road condition [7]. The utilization of feedback control has been proven over the years as a good mechanism that could be used to improve the performance of the control system [8]. In this regard, various attempts have been made to apply different feedback controller frameworks for suspension systems to achieve a better ride comfort. In the context of linear models, Sam et al. [9] proposed a robust strategy based on Proportional-Integral Sliding Mode Control (PI-SMC). A quarter-car model is used in the study. The mathematical model of the suspension system is presented in a state space formulation. The results of the PI-SMC controller show a better performance compared to the Linear Quadratic Regulator (LQR) method and the passive suspension system. Another application of SMC into the suspension system was implemented by [2, 4].

Zhou [2] developed an optimal SMC to improve the dynamic quality of SMC control for an active suspension system. Genetic Algorithm (GA) is introduced to tune the weight coefficients of the SMC's control law. The simulation results show that the optimal SMC based on GA controller has better control performance than the traditional SMC controller. Zhang [4] presented a feed-forward and feedback SMC for active suspension systems based on quarter-car model. Based on reading some state variables of the suspension system, an analytic term and a disturbances compensation term are developed to improve the performance of the SMC. The result of a numerical example is shown that proposed feed-forward and feedback SMC has a better effect to attenuate the random road surface disturbances than traditional SMC controller. In addition, Salem and Aly [10] presented a comparative study between the PID controller and a Fuzzy Logic Controller (FLC) to control an active suspension system. The outcomes showed that the FLC provides good results compared to those of the PID controller. Moreover, Romsai et al. [11] proposed an optimized approach for the classical PID controller based on Lévy-flight intensified current search optimization approach.

Recently, Al-Khazraji [3] presented a Proportional-Derivative State Feedback (PDSF) controller approach. Two meta-heuristic optimizations named Bees Algorithm (BA) and Grey Wolf Optimization (GWO) are proposed to optimize the feedback gain matrix of the PDSF controller based on the Integral Time of Absolute Error (ITAE) index. The results show the superiority of the BA-based PDSF controller in terms of reducing the ITAE index in comparison with the results obtained from GWO based PDSF. Abut and Salkim [12] presented a comparative study between Linear Quadratic Regulator (LQR), FLC, and fuzzy-LQR control algorithms to the suspension system for active control. It was found that the car's ride comfort has been significantly improved by the fuzzy-LQR control method. An LQR control strategy utilizing Ant Colony Optimization (ACO) in the active suspension system was presented by Manna et al. [13]. They used it in an experimental setting on a quarter-car model. In three track profiles, the suggested approach was experimentally contrasted with the traditional LQR and Model Predictive Control (MPC) approaches. In comparison to the classically tuned LQR and MPC, the results demonstrated that the proposed method significantly reduced the acceleration of the body due to uneven road profiles. It has also been demonstrated to greatly enhance vehicle handling and passenger comfort.

For more reasonable representation of the real system, many papers have considered the nonlinearity in the modeling of the suspension system. In this direction, Aldair et al. [14] presented an optimized Fractional Order PID (FOPID) controller for a nonlinear active suspension system. Sadeghi et al. [15] developed a nonlinear PD controller approach for a nonlinear quarter car suspension system. The proposed controller is compared with the results of a fuzzy-PID controller show that the proposed controller is more stable and has less damping in response while the system speed is improved. In another work, Nagarkar et al. [16] compared the performance of the PID controller and that of the LQR controller in controlling the nonlinear suspension system. Sun et al. [17] proposed an adaptive backstepping control scheme for nonlinear suspension systems to improve ride comfort in the presence of parametric uncertainties. Liu et al. [18] proposed an adaptive sliding fault tolerant controller to stabilize a nonlinear active suspension system. Differential evolution (DE) algorithm and linear matrix inequalities (LMIs) are introduced to design appropriate parameters of the sliding surface. Simulation results illustrate the effectiveness of the proposed strategy. Zhao et al. [19] proposed a dual adaptive robust controller (ARC) for a nonlinear active suspension system. The tunable parameters in the control law are optimized by solving LMI with kidney-inspired algorithm. The effectiveness and robustness of the proposed controller are demonstrated via excessive simulation experiments over different road conditions.

In the above-mentioned literature, some of the limitations still available for practical implementation are described as follows:

- Studying the effect of the nonlinearities in the damper and the spring of the suspension system has not extensively considered.
- The challenging to provide comfort ride and stability performance with the presence of the actuator saturation is not extensively considered.
- The mismatched uncertainty in the mass of the car body has not extensively considered.

To address these limitations, this study proposes and compares the performance of two control frameworks including the PID controller and the SF controller. In this context, determining the two controllers' design variables to generate control signals that make the nonlinear system follow a desired performance is a very challenging task. In particular, many authors choose to utilize metaheuristic optimization methods to find the best controller adjustable parameters since they are more

effective than using the trial-and-error method [20-23]. The metaheuristic algorithms have been successfully applied to solve a wide range of optimization-related problems [24-27]. To address the tuning problem in this work, the recent Swarm Bipolar Algorithm (SBA) has been employed.

To end this, the rest of this paper is organized as follows: Section 2 gives the mathematical model of the nonlinear active suspension system. In Section 3, the PID and SF controllers have been explained. Section 4 presents the SBA. The validation of the proposed optimized controllers is reported in the Section 5 and finally, the conclusion is summarized in Section 6.

2. System modeling

First, the mathematical model of the active suspension system is given in this section. The active suspension system can be represented by the 2DOF Mass-Spring-Damper (MSD) system, as illustrated in Fig. 1 [9] in which m_b and m_w are the masses of the car body and the wheel, respectively, F_s, F_d, F_a and F_t are the forces that are generated by the wheel spring, the wheel damper, the actuator, and the spring of the tire, respectively, d is the road disturbance, x_1 and x_2 are the positions of the car body and the wheel, respectively, \dot{x}_3 and \dot{x}_4 are the velocities of the car body and the wheel, respectively, and \ddot{x}_3 and \ddot{x}_4 are the acceleration variables of the car body and the wheel, respectively.

Based on the Newton's law, the motion equation for the masses of the car body and the wheel are given by [11]:

$$m_b \ddot{x}_3 = -F_s - F_d + F_a \tag{1}$$

$$m_w \ddot{x}_4 = F_s + F_d - F_a - F_t \tag{2}$$

The nonlinear force (F_s) is computed as follows [16] [28]:

$$F_s = k_{sl}(x_1 - x_2) + k_{sn}(x_1 - x_2)^3 \tag{3}$$

The nonlinear force (F_d) is computed as follows [18] [19]:

$$F_d = c_{dl}(\dot{x}_1 - \dot{x}_2) + c_{sn}(\dot{x}_1 - \dot{x}_2)^2 \tag{4}$$

The force (F_t) is computed as follows [16] [18]:

$$F_t = k_t(x_2 - d) \tag{5}$$

where $k_{sl}, k_{sn}, c_{dl}, c_{sn}$, and k_t are the linear

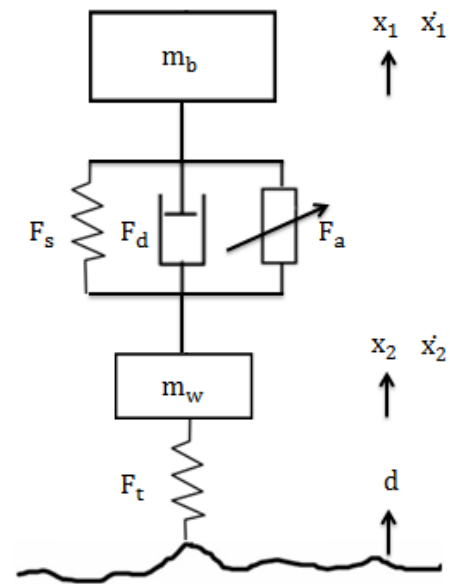


Figure. 1 Active suspension system

stiffness coefficient of the spring, the nonlinear stiffness coefficient of the spring, the linear damper coefficient of the spring, the nonlinear damper coefficient of the spring, and the stiffness coefficient of the spring in the tire. By substituting Eqs. (3) and (4) into Eqs. (1) and (2), we obtain:

$$m_b \ddot{x}_3 = -(k_{sl}(x_1 - x_2) + k_{sn}(x_1 - x_2)^3) - (c_{dl}(\dot{x}_1 - \dot{x}_2) + c_{sn}(\dot{x}_1 - \dot{x}_2)^2) + F_a \tag{6}$$

$$m_w \ddot{x}_4 = (k_{sl}(x_1 - x_2) + k_{sn}(x_1 - x_2)^3) + (c_{dl}(\dot{x}_1 - \dot{x}_2) + c_{sn}(\dot{x}_1 - \dot{x}_2)^2) - F_a - (k_t(x_2 - d)) \tag{7}$$

For the purpose of the control design, the state variable equations of the nonlinear suspension system are defined as:

$$\dot{x}_1 = x_3 \tag{8}$$

$$\dot{x}_2 = x_4 \tag{9}$$

$$\dot{x}_3 = \frac{1}{m_b} \left(-(k_{sl}(x_1 - x_2) + k_{sn}(x_1 - x_2)^3) - (c_{dl}(\dot{x}_1 - \dot{x}_2) + c_{sn}(\dot{x}_1 - \dot{x}_2)^2) + F_a \right) \tag{10}$$

$$\dot{x}_4 = \frac{1}{m_w} \left((k_{sl}(x_1 - x_2) + k_{sn}(x_1 - x_2)^3) + (c_{dl}(\dot{x}_1 - \dot{x}_2) + c_{sn}(\dot{x}_1 - \dot{x}_2)^2) - F_a - (k_t(x_2 - d)) \right) \tag{11}$$

3. Controller design

In this section, the details and the procedure of designing the PID controller and the SF controller for the nonlinear suspension system are presented. These controllers designed for the suspension system aim to increase car handling and passenger comfort by reducing the vibrations that occur in passive suspension systems. Specifically, the PID and the SF controllers are frequently engaged in controlling linear systems, where the PID controller design parameters can be found using the classical techniques, such as Ziegler-Nichols method for the PID controller and the pole placement method for the SF controller. However, to utilize these controllers for nonlinear systems, the system is required to be linearized around an operation point. However, this approach could be practically applied for systems that have a small region of operation [29]. To overcome this restriction, in this paper, the swarm optimization is proposed to handle the tuning process of the PID and the SF controllers' design variables for the nonlinear suspension system.

3.1 The PID controller

The PID controllers have been successfully implemented in various control design problems [30-31]. The objective of the PID controller design is to manipulate the dynamic of the system to maintain the system in a stable state and/or reach a desired state [32]. Particularly, the control action (u) of the PID controller results from the summation of three terms, as shown in Fig. 2.

After measuring the output (y) of the process, the error (e) is determined by subtracting the reference (i.e. the desired output) (y_r) from the measured output (y). Then, the proportional term adjusts u based on the weighted gain K_p of e of the process. Moreover, the integral term adjusts u based on the weighted gain K_i of the integration of the process error. Finally, the derivative term adjusts u based on the weighted gain K_d of the rate of change of the

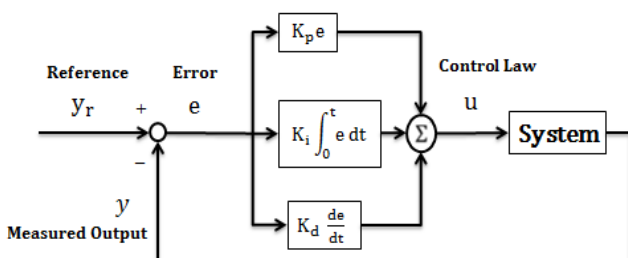


Figure. 2 The System with the PID controller

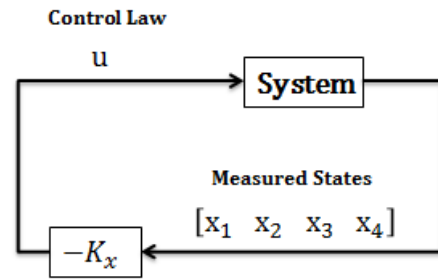


Figure. 3 The system with the SF controller

process error. The final control law of the PID controller is defined as follows [33, 34]:

$$u = K_p e + K_i \int_0^t e \, dt + K_d \frac{de}{dt} \tag{12}$$

3.2 State feedback controller

The SF controller is a promising approach to design a controller, provided that the states of the system are measurable and that the system is controllable. The SF controller shapes the response of the system by adjusting the system poles' location towards the desired location [35]. The SF controller is depicted in Fig. 3.

The control action u of the SF controller is computed based on the matrix gains K_x of the system states, as given below [36]:

$$u(t) = - \begin{bmatrix} K_{x1} \\ K_{x2} \\ K_{x3} \\ K_{x4} \end{bmatrix} [x_1 \ x_2 \ x_3 \ x_4] \tag{13}$$

4. Swarm bipolar algorithm

Optimization is a work to find the most appropriate or acceptable solution among the set of solution candidates for a defined problem. Optimization is essential and critical in the real world, especially in the engineering and industrial fields [37]. In many optimization studies, the set of solution candidates is limited to the defined constraints. In other terms, these constraints are also called hard constraints. Meanwhile, the quality of the chosen solution is measured by using the objective function [38], also called soft constraints. Meanwhile, the decision variables construct the solution set and are used in the objective function. These three aspects (constraints, accuracy, and decision variables) are fundamental to any optimizations [39].

In this work, the tuning process of the PID and the SF controllers is formulated as an optimization problem, as opposed to the case of using the trial-and-error method, which is a time-consuming method. Subsequently, the optimization problem is solved by applying the swarm bipolar algorithm (SBA) technique. The SBA is a meta-heuristic optimization technique introduced by Kusuma and Dinimaharawati [40] in 2024.

As its name suggests, SBA is constructed based on swarm intelligence to consist of a certain number of autonomous agents. The bipolar term comes from the concept that the swarm is split into two equal-sized sub-swarms as shown in Fig. 4. In Fig. 4, the first sub-swarm is colored red, while the second sub-swarm is colored green. The objective of splitting the swarm and introducing multiple references as proposed in this work is to diversify the motion of the swarm. This diversification is designed to improve the exploration capability so that it can help the swarm to escape from the local optimal. Some swarm members may move toward the local optimal, but the others may move to other alternatives [40].

The pseudo code of the SBA is given in Algorithm1. During the initialization phase, all swarm members are distributed uniformly within the search space as given in Eq. (13). It means that the sub swarm members are also distributed uniformly

within the search space. Four directed searches are performed sequentially by each swarm member in each loop of iteration. The first search is the search toward the finest swarm member as given in Eqs. (17) and (18). The second search is the search for the finest sub-swarm member as given in Eqs. (19) and (18). Each sub-swarm member follows its own finest sub-swarm member. The third search is the search toward the middle between the two finest sub-swarm members as given in Eqs. (20) and (18). The fourth search is the search relative to a randomly picked sub-swarm member from the opposite sub-swarm as given in Eqs. (21), (22) and (18). The illustration of these four searches is presented in Fig. 5.

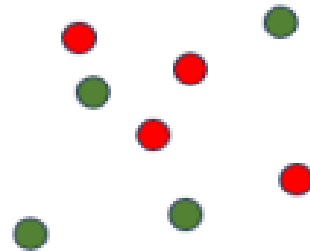


Figure. 4 Illustration of two equal size sub swarms

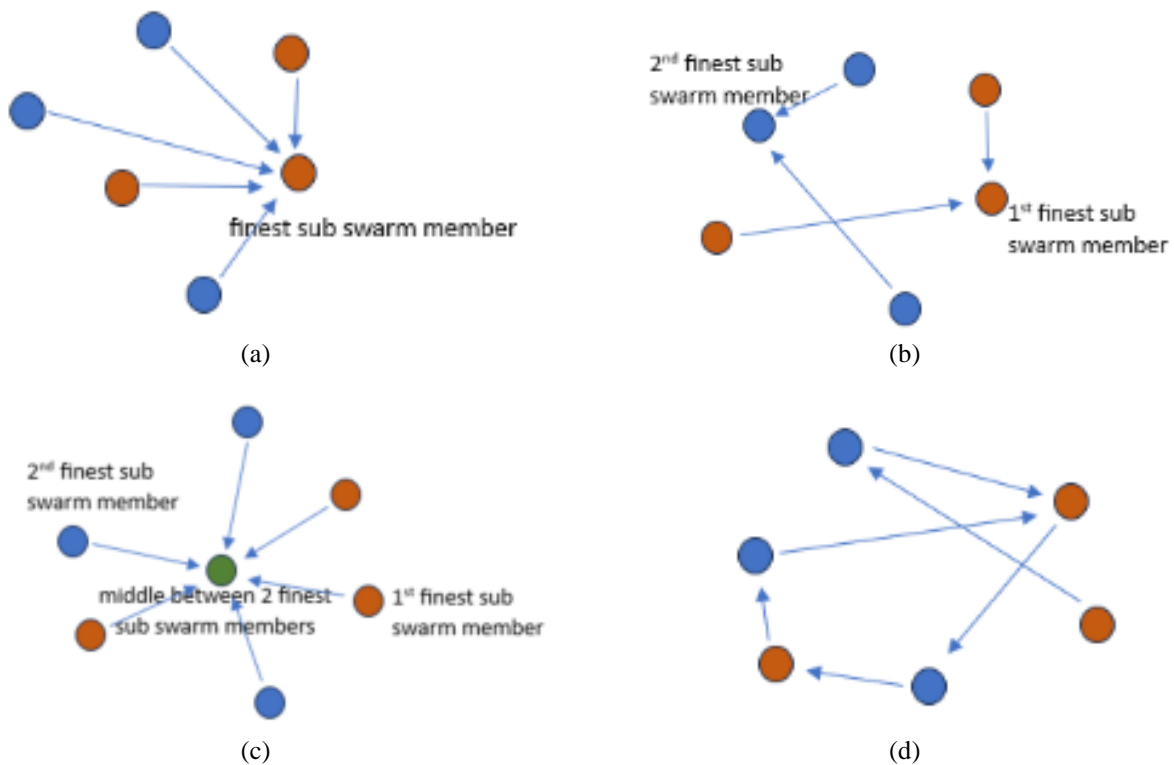


Figure. 5 Illustration of four searches: (a) first search, (b) second search, (c) third search, and (d) fourth search

Algorithm I: SBA's pseudo code

```

1  begin
2  for each  $s \in S$  do
3    generate initial solution using Eq. (13)
4    update  $s_b$  and  $s_{sb}$  using Eq. (14) to Eq. (15)
5  end for
6  for  $t = 1$  to  $t_m$  do
7    for each  $s \in S$  do
8      first search using Eq. (17) and Eq. (18)
9      update  $s_b$  and  $s_{sb}$  using Eq. (14) to Eq. (16)
10     second search using Eq. (19) and Eq. (18)
11     update  $s_b$  and  $s_{sb}$  using Eq. (14) to Eq. (16)
12     third search using Eq. (20) and Eq. (18)
13     update  $s_b$  and  $s_{sb}$  using Eq. (14) to Eq. (16)
14     fourth search using Eq. (21), Eq. (22), Eq. (18)
15     update  $s_b$  and  $s_{sb}$  using Eq. (14) to Eq. (16)
16   end for
17 end for
18 return  $s_b$ 
19 end
    
```

$$s_{i,j} = s_{b,j} + r_1(s_{u,j} - s_{i,j}) \tag{13}$$

$$s'_b = \begin{cases} s_i, f(s_i) < f(s_b) \\ s_b, \text{else} \end{cases} \tag{14}$$

$$s'_{b1} = \begin{cases} s_i, f(s_i) < f(s_{sb1}) \wedge 1 \leq i \leq \frac{n(s)}{2} \\ s_{sb1}, \text{else} \end{cases} \tag{15}$$

$$s'_{b2} = \begin{cases} s_i, f(s_i) < f(s_{sb2}) \wedge \frac{n(s)}{2} < i \leq n(s) \\ s_{sb2}, \text{else} \end{cases} \tag{16}$$

$$c_{i,j} = s_{i,j} + r_1(s_{b,j} - r_2s_{i,j}) \tag{17}$$

$$s'_i = \begin{cases} c_i, f(c_i) < f(s_i) \\ s_i, \text{else} \end{cases} \tag{18}$$

$$c_{i,j} = \begin{cases} s_{i,j} + r_1(s_{sb1,j} - r_2s_{i,j}), 1 \leq i \leq \frac{n(s)}{2} \\ s_{i,j} + r_1(s_{sb2,j} - r_2s_{i,j}), \frac{n(s)}{2} \leq i \leq n(s) \end{cases} \tag{19}$$

$$c_{i,j} = s_{i,j} + r_1\left(\frac{s_{sb1,j} + s_{sb2,j}}{2} - r_2s_{i,j}\right) \tag{20}$$

$$s_t = \begin{cases} U(s_1, s_{\frac{n(s)}{2}}), \frac{n(s)}{2} \leq i \leq n(s) \\ U(s_{\frac{n(s)}{2}+1}, s_n(s)), 1 \leq i \leq \frac{n(s)}{2} \end{cases} \tag{21}$$

$$c_{i,j} = \begin{cases} s_{i,j} + r_1(s_{t,j} - r_2s_{i,j}), f(s_t) < f(s_i) \\ s_{i,j} + r_1(s_{i,j} - r_2s_{t,j}), \text{else} \end{cases} \tag{22}$$

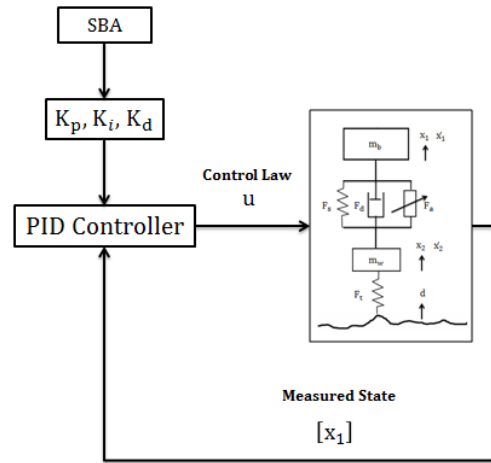


Figure. 6 Proposed PID controller tuned by SBA

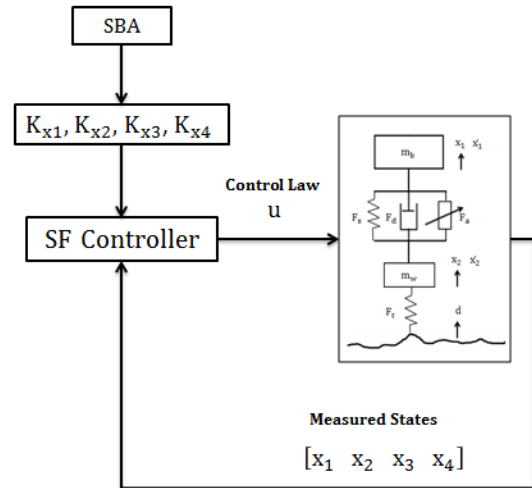


Figure. 7 Proposed SF controller tuned by SBA

Table 1. Quarter car active suspension system parameters

Parameters	Value
Body mass (m_b)	290 Kg
Wheel mass (m_w)	59 Kg
Linear stiffness of the spring (k_{sl})	14500 N/m
Nonlinear stiffness of the spring (k_{sn})	160000 N/m ³
Stiffness of the tire spring (k_t)	190000 N/m
Linear damping factor of the damper (c_l)	1385.4 Ns/m
Nonlinear damping factor of the damper (c_n)	170 Ns ² /m ²

Table 2. Parameters of road profile

Parameter	Value
A_m	0.1 m
L_m	5 m
v_c	45 km/h
t_{sim}	4 s

5. Computer simulation results

In this section, the simulation results of the PID and the SF controllers to control the nonlinear suspension system utilizing MATLAB are presented. The system's parameters are provided in Table 1 [18]. The configuration of the PID and SF controllers based SBA optimization are shown in Figs. 6 and 7. The profile of the road disturbance is represented as [18]:

$$d = \begin{cases} \frac{A_m}{2} \left(1 - \cos\left(\frac{2\pi t_{sim}}{\delta}\right) \right), & 0 \leq t_{sim} \leq \delta \\ 0, & otherwise \end{cases} \quad (23)$$

where t_{sim} is the simulation time, A_m is the amplitude of the bump, δ is a coefficient computed based on the length (L_m) of the bump and the forward velocity of the car (v_c) as follows:

$$\delta = \frac{L_m}{v_c} \quad (24)$$

The numerical value of the road profile is reported in Table 2.

Eqs (8)-(11) are used to simulate the dynamics of the suspension system. The Root Mean Square Error (RMSE) criterion was selected as a cost function for the SBA to improve the performance of the PID and the SF controllers. This RMSE index is given by [41]:

$$RMSE = \sqrt{\frac{1}{n} \sum_{m=1}^n e_m^2} \quad (25)$$

where e_m is the error between the body mass position x_1 and the desired position (i. e. $x_d = 0$).

It must be pointed out that the input force of the actuator to the suspension system is saturated by ± 800 N. As a result, the tuning process of the controllers based on the SBA for the nonlinear suspension system can be formulated as an optimization problem, as follows [3]:

$$\begin{aligned} & \text{minimize } RMSE(\text{var}) \\ & \text{s. t} \\ & -800 \geq u \geq 800 \end{aligned} \quad (26)$$

where RMSE is the objective function that needs to be minimized. The decision vectors (var) are the PID controller's gains (K_p , K_i and K_d), as given in Eq. (12) and the SF controller's feedback gain matrix (K_{x1} , K_{x2} , K_{x3} , and K_{x4}), as given in Eq. (13). The parameters of the SBA are provided in Table 3. The best setting of the SBA parameters is selected after

repeating the simulation several times with different values until achieving the desired control performance.

Table 3. SBA's parameters

Parameter	Value
Population size (N)	25
Number of iterations (T_{max})	35
Coefficient value (a)	2

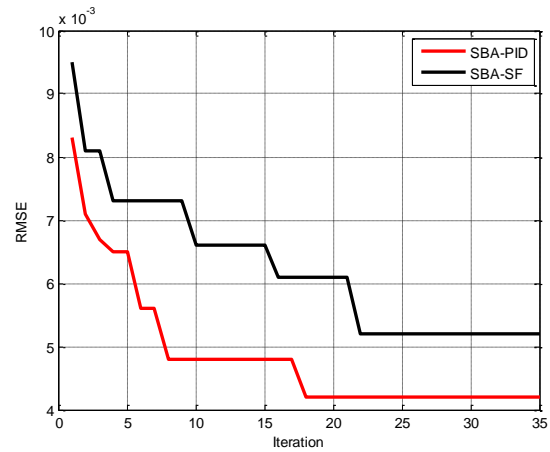


Figure. 8 SBA's convergence for the SF and the PID controllers without actuator saturation

Table 4. Optimal setting of the controllers without actuator saturation

Controller	Parameters	Values
SBA-PID	K_p	762
	K_i	620
	K_d	1290
SBA-SF	K_{x_1}	6240
	K_{x_2}	3720
	K_{x_3}	4850
	K_{x_4}	400

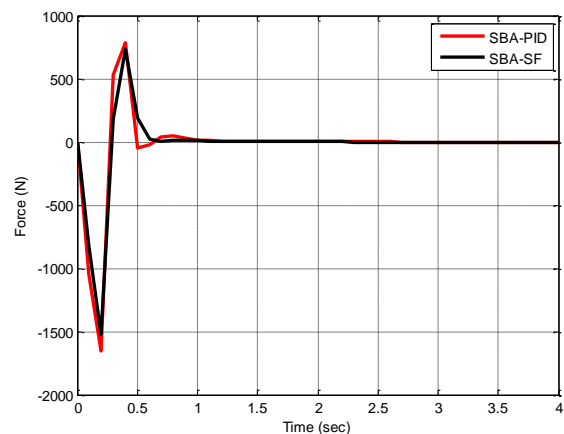


Figure. 9 Control law of the controllers without actuator saturation

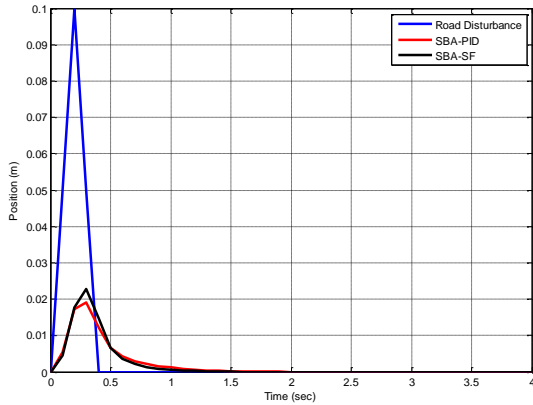


Figure. 10 Suspension system response without actuator saturation

Table 5. Performance comparison without actuator saturation

Index	SBA-PID	SBA-SF	Ref. [18]
RMSE	0.0042	0.0052	0.013
Max(x_1)	0.019	0.022	0.025

5.1 Scenario1: without actuator saturation

For the purpose of comparison with the results of paper [18], in this subsection the saturation limit of the control input u will not impose a constraint in the optimization problem as given in Eq. (26). The convergence behaviour of the SBA is shown in Fig. 8. The values of the designed parameters for the PID and the SF controllers are given in Table 4. Figs. 9 and 10 illustrate the control law and the response of the two controlled systems, respectively. The corresponding numerical value of the RMSE index and the maximum car body displacement $Max(x_1)$ are reported in Table 5.

It can be seen from Table 5 the two measured including the RMSE index and the value $Max(x_1)$ are improved by the SBA-PID and SBA-SF in comparison with the result in Ref. [18]. The percentage of improvement in the RMSE index was 67.7% for the SBA-PID and 60% for the SBA-SF. Moreover, the improvement in the value $Max(x_1)$ was 24% for the SBA-PID and 12% for SBA-SF.

5.2 Scenario1: with actuator saturation

The limitations of actuators commonly cause the control input saturate. Actuator saturation affects almost all practical control systems [42]. In this subsection the saturation limit of the control input u imposes a constraint in the optimization problem as

given in Eq. (26). In this regard, the convergence behaviour of the SBA is shown in Fig. 11. The values of the designed parameters for the PID and the SF controllers are given in Table 6. Figs. 12 and 13 illustrate the control law and the response of the two controlled systems, respectively. The corresponding numerical value of the RMSE index and the $Max(x_1)$ value are reported in Table 7.

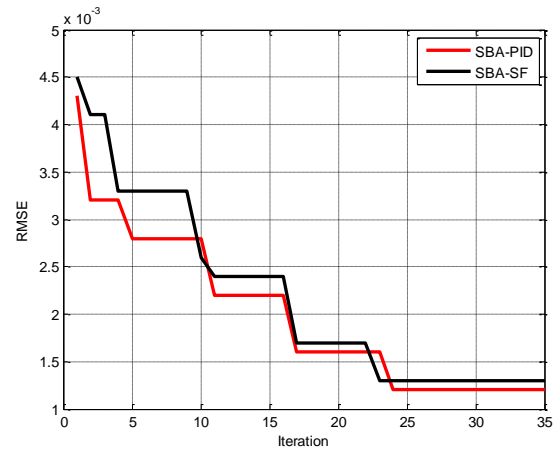


Figure. 11 SBA's convergence for the SF and the PID controllers with actuator saturation

Table 6. Optimal setting of the controllers

Controller	Parameters	Values
PID Controller	K_p	2850
	K_i	50
	K_d	1900
SF Controller	K_{x_1}	4840
	K_{x_2}	1420
	K_{x_3}	950
	K_{x_4}	100

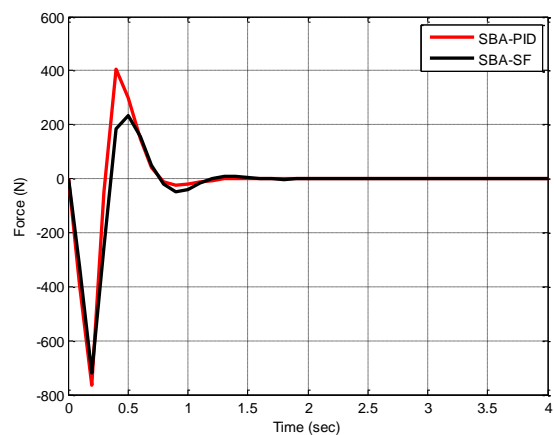


Figure. 12 Control law of the controllers with actuator saturation

From Fig. 11, it can be observed that the control signals for the two controllers are within the acceptable force range of the actuator. Moreover, in Fig. 12, it can be seen that the SBA-PID controller has achieved better performance than that of the SBA-SF. This result can be validated numerically from Table 7, where it is obvious that the value of the RMSE index for the SBA-PID controller (0.012) is less than the value of the RMSE index for the SBA-SF controller (0.013). Moreover, the value $\text{Max}(x_1)$ of the SBA-PID is 0.054 which is less than the value $\text{Max}(x_1)$ of the SBA-PID which is 0.056.

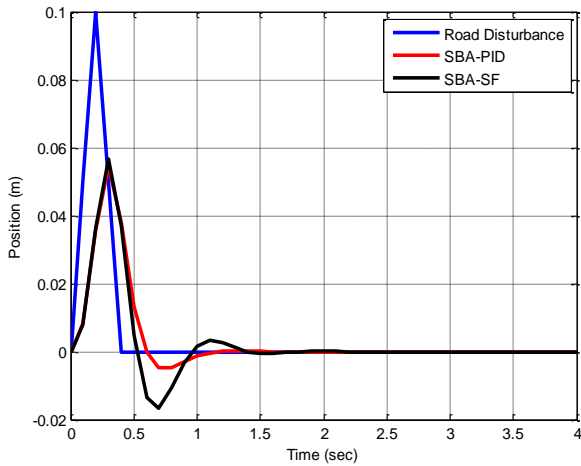


Figure. 13 Suspension system response with actuator saturation

Table 7. Performance comparison with actuator saturation

Index	SBA-PID	SBA-SF
RMSE	0.012	0.013
$\text{Max}(x_1)$	0.054	0.056

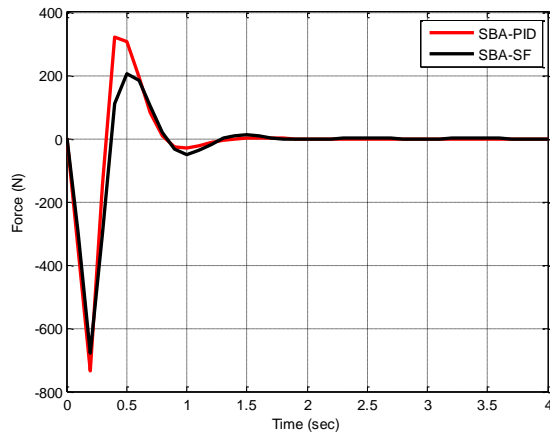


Figure. 14 Control law of the controllers when the mass of the car body increased by 20%

In practical, the mass of the car body varies with the number of passengers in a car. Therefore, to evaluate the robustness of the two controllers against the uncertainty in the mass of the car body, it was assumed that the mass of the car body is changed by $\pm 20\%$ of its value. Figs. 14 and 15 show the control law and the response of the two controlled systems when the mass of the car body is increased by 20%, respectively. The corresponding numerical value of the RMSE index and the value $\text{Max}(x_1)$ are reported in Table 8.

Figs. 16 and 17 show the control law and the response of the two controlled systems when the mass of the car body is decreased by 20%, respectively. The corresponding numerical value of the RMSE index and the value $\text{Max}(x_1)$ are reported in Table 9.

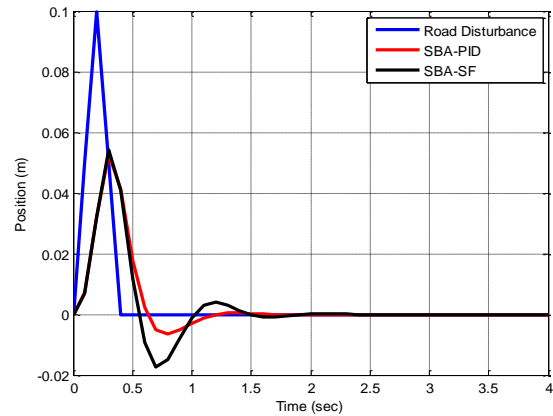


Figure. 15 Suspension system response when the mass of the car body increased by 20%

Table 8. Performance comparison when the mass of the car body increased by 20%

Index	SBA-PID	SBA-SF
RMSE	0.012	0.013
$\text{Max}(x_1)$	0.054	0.056

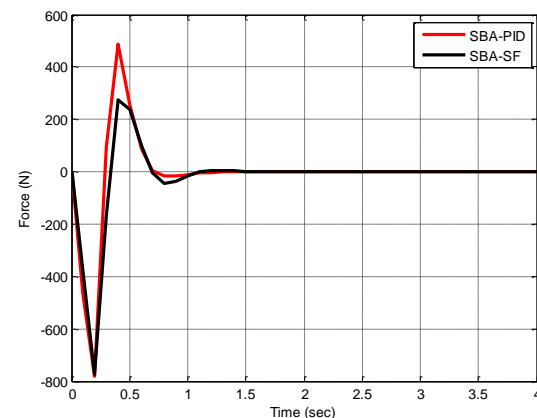


Figure. 16 Control law of the controllers when the mass of the car body decreased by 20%

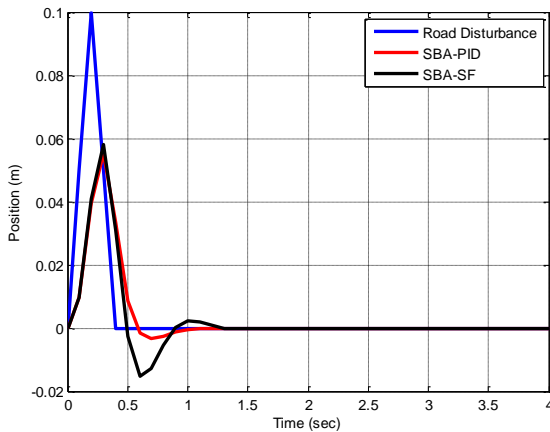


Figure. 17 Suspension system response when the mass of the car body decreased by 20%

Table 9. Performance comparison when the mass of the car body decreased by 20%

Index	SBA-PID	SBA-SF
RMSE	0.012	0.013
Max(x ₁)	0.054	0.056

It can be revealed based on Figs. 14 and 16 that the control signal for the two controllers with the two cases is within the acceptable force range of the actuator. Moreover, in Figs 15 and 17, it can be seen that the SBA-PID controller has achieved better performance than that of the SBA-SF. This result can be validated numerically from Tables 8 and 9. Table 8 illustrates that the value of the RMSE index for the SBA-PID controller (0.12) is less than the value of the RMSE index for the SBA-SF controller (0.013) in the case when the mass of the car body is increased by 20%. Moreover, the value $Max(x_1)$ of the SBA-PID is 0.054 which is less than the value $Max(x_1)$ of the SBA-PID which is 0.056. Table 9 illustrates that the value of the RMSE index for the SBA-PID controller (0.012) is less than the value of the RMSE index for the SBA-SF controller (0.013) in the case when the mass of the car body is decreased by 20%. Moreover, the value $Max(x_1)$ of the SBA-PID is 0.054 which is less than the value $Max(x_1)$ of the SBA-PID which is 0.056.

These results sufficiently indicate that the SBA-PID controller has stronger robustness in improving vehicle body stability and ride comfort in the presence of the uncertainty in the mass of the car body.

6. Conclusion

The goal of the suspension system is to isolate the car-body from the road irregularities while improving

the road-holding characteristics. After a survey of the previous research studies on the controlled suspension system, it was observed that the majority of these studies are limited to linear model and/or without considering the saturation in the actuator. To address the nonlinearities and actuator saturation in controlling the suspension system, this paper proposed a designing of the PID controller and the SF controller to act as the active controllers for the suspension system. The two controllers' parameters were tuned using a recent development algorithm named swarm bipolar algorithm (SBA) technique based on minimizing the RMSE index. The numerical simulation results using MATLAB show that the RMSE of the SBA-PID controller is less than the RMSE of the SBA-SF controller, which leads to improve the ride comfort.

Notation list:

d	Dimension
f	objective function
i	index for swarm member
j	index for dimension
s	swarm member
S	population size
s _l	lower boundary
s _u	upper boundary
s _b	the finest swarm member
s _{sb}	the finest sub swarm member
s _t	randomly picked swarm member
r ₁	floating point uniform random [0,1]
r ₂	integer uniform random [1,2]
t	Iteration
t _m	maximum iteration
U	uniform random

Conflicts of Interest

The authors declare no conflict of interest.

Author Contributions

Conceptualization, Mohammed A. AL-Ali, Omar F. Lutfy and Huthaifa Al-Khazraj; methodology, Mohammed A. AL-Ali, Omar F. Lutfy and Huthaifa Al-Khazraj; software, Mohammed A. AL-Aali and Huthaifa Al-Khazraj; validation, Mohammed A. AL-Ali and Omar F. Lutfy; formal analysis, Mohammed A. AL-Ali, Omar F. Lutfy and Huthaifa Al-Khazraj; investigation, Mohammed A. AL-Ali and Huthaifa Al-Khazraj; resources, Mohammed A. AL-Ali; data creation, Mohammed A. AL-Ali; writing—original draft preparation, Mohammed A. AL-Ali and Huthaifa Al-Khazraj; writing—review and editing,

Omar F. Lutfy; visualization, Mohammed A. AL-Ali; supervision, Omar F. Lutfy and Huthaifa Al-Khazraj; project administration, Omar F. Lutfy.

References

- [1] K. D. Rao, and S. Kumar, "Modeling and simulation of quarter car semi active suspension system using LQR controller", *Advances in Intelligent Systems and Computing*, pp. 441-448, 2015.
- [2] C. Zhou, X. Liu, W. Chen, F. Xu, and B. Cao, "Optimal sliding mode control for an active suspension system based on a genetic algorithm," *Algorithms*, Vol. 11, No. 12, p. 205, 2018.
- [3] H. Al-Khazraji, "Optimal design of a Proportional-Derivative State Feedback controller based on meta-heuristic optimization for a quarter car suspension system", *Math. Model. Eng. Probl.*, Vol. 9, No. 2, pp. 437-442, 2022.
- [4] B. L. Zhang, G. Y. Tang, and F. L. Cao, "Optimal sliding mode control for active suspension systems", In: *Proc. of 2009 International Conf on Networking, Sensing and Control*, 2009.
- [5] M. Nagarkar, and G. J. V. Patil, "Optimization of the linear quadratic regulator (LQR) control quarter car suspension system using genetic algorithm", *Ing. Investig.*, Vol. 36, No. 1, pp. 23-30, 2016.
- [6] F. Yakub, P. Muhammad, Z. H. C. Daud, A. Y. A. Fatah, and Y. Mori, "Ride comfort quality improvement for a quarter car semi-active suspension system via state-feedback controller", In: *Proc. of 2017 11th Asian Control Conf (ASCC)*, 2017.
- [7] R. Bai, and D. Guo, "Sliding-mode control of the active suspension system with the dynamics of a hydraulic actuator", *Complexity*, Vol. 2018, pp. 1-6, 2018.
- [8] H. Al-Khazraji, C. Cole, and W. Guo, "Dynamics analysis of a production-inventory control system with two pipelines feedback", *Kybernetes*, Vol. 46, No. 10, pp. 1632-1653, 2017.
- [9] Y. M. Sam, J. H. S. Osman, and M. R. A. Ghani, "A class of proportional-integral sliding mode control with application to active suspension system", *Syst. Control Lett.*, Vol. 51, No. 3-4, pp. 217-223, 2004.
- [10] M. M. Salem, and A. A. Aly, "Fuzzy control of a quarter-car suspension system", *International Journal of Computer and Information Engineering*, Vol. 3, No. 5, pp. 1276-1281, 2009.
- [11] W. Romsai, A. Nawikavatan, and D. Puangdownreong, "Application of Lévy-flight intensified current search to optimal PID controller design for active suspension system", *International Journal of Innovative Computing, Information and Control*, Vol. 17, No. 2, pp. 483-497, 2021.
- [12] T. Abut, and E. Salkim, "Control of quarter-car active suspension system based on optimized fuzzy linear quadratic regulator control method", *Applied Sciences*, Vol. 13, No. 15, 2023.
- [13] S. Manna et al., "Ant colony optimization tuned closed-loop optimal control intended for vehicle active suspension system", *IEEE Access*, Vol. 10, pp. 53735-53745, 2022.
- [14] A. A. Aldair, and W. J. Wang, "Design of fractional order controller based on evolutionary algorithm for a full vehicle nonlinear active suspension systems", *International Journal of Control and Automation*, Vol. 3, No. 4, pp. 33-46, 2010.
- [15] M. S. Sadeghi, F. Bavafa, S. M. S. Alavi, and S. Varzandian, "Nonlinear PD controller design for a nonlinear quarter car suspension system", In: *Proc. of the 2nd International Conf on Control, Instrumentation and Automation*, 2011.
- [16] M. P. Nagarkar, Y. J. Bhalerao, G. J. V. Patil, and R. N. Z. Patil, "Multi-objective optimization of nonlinear quarter car suspension system - PID and LQR control", *Procedia Manuf.*, Vol. 20, pp. 420-427, 2018.
- [17] W. Sun, H. Pan, Y. Zhang, and H. Gao, "Multi-objective control for uncertain nonlinear active suspension systems", *Mechatronics (Oxf.)*, Vol. 24, No. 4, pp. 318-327, 2014.
- [18] S. Liu, H. Zhou, X. Luo, and J. Xiao, "Adaptive sliding fault tolerant control for nonlinear uncertain active suspension systems", *J. Franklin Inst.*, Vol. 353, No. 1, pp. 180-199, 2016.
- [19] D. Zhao, M. Du, T. Ni, M. Gong, and L. Ma, "Dual adaptive robust control for uncertain nonlinear active suspension systems actuated by asymmetric electrohydraulic actuators", *Low Freq. Noise Vibr.*, Vol. 40, No. 3, pp. 1607-1632, 2021.
- [20] H. AL-Khazraji, C. Cole, and W. Guo, "Optimization and simulation of dynamic performance of production-inventory systems with multivariable controls", *Mathematics*, Vol. 9, No. 5, p. 568, 2021.
- [21] N. M. Noaman, A. S. Gatea, A. J. Humaidi, S. K. Kadhim, and A. F. Hasan, "Optimal tuning of PID-controlled magnetic bearing system for tracking control of pump impeller in artificial

- heart”, *Journal Européen des Systèmes Automatisés*, Vol. 56, No. 1, 2023.
- [22] A. K. Hamoudi, and L. T. Rasheed, “Design and implementation of adaptive backstepping control for position control of propeller-driven pendulum system”, *J. Eur. Syst. Autom.*, Vol. 56, No. 2, pp. 281-289, 2023.
- [23] H. Al-Khazraji, R. M. Naji, and M. K. Khashan, “Optimization of Sliding Mode and Back-Stepping Controllers for AMB Systems Using Gorilla Troops Algorithm”, *Journal Européen des Systèmes Automatisés*, Vol. 57, No. 2, pp. 417-424, 2024.
- [24] H. Al-Khazraji, “Industrial picking and packing problem: Logistic management for products expedition”, *Journal of Mechanical Engineering Research and Developments*, Vol. 43, No. 2, pp. 74-80, 2020.
- [25] H. Al-Khazraji, S. Khlil, and Z. Alabacy, “Cuckoo Search Optimization for solving Product Mix Problem”, *IOP Conf. Ser. Mater. Sci. Eng.*, Vol. 1105, No. 1, p. 012016, 2021.
- [26] H. AL-Khazraji, A. Nasser, and S. Khlil, “An intelligent demand forecasting model using a hybrid of metaheuristic optimization and deep learning algorithm for predicting concrete block production”, *IAES Int. J. Artif. Intell. (IJ-AI)*, Vol. 11, No. 2, p. 649, 2022.
- [27] H. Al-Khazraji, “Comparative study of whale optimization algorithm and flower pollination algorithm to solve workers assignment problem”, *Int. J. Prod. Manag. Eng.*, Vol. 10, No. 1, pp. 91-98, 2022.
- [28] D. Koulocheris, G. Papaioannou, and D. Christodoulou, “Assessment of the optimization procedure for the nonlinear suspension system of a heavy vehicle”, *Mobility and Vehicle Mechanics*, Vol. 42, No. 2, pp. 17-35, 2016.
- [29] A. K. Ahmed, and H. Al-Khazraji, “Optimal control design for propeller pendulum systems using gorilla troops optimization”, *J. Eur. Syst. Autom.*, Vol. 56, No. 4, pp. 575-582, 2023.
- [30] H. AL-Khazraji, C. Cole, and W. Guo, “Analysing the impact of different classical controller strategies on the dynamics performance of production-inventory systems using state space approach”, *J. Model. Manag.*, Vol. 13, No. 1, pp. 211-235, 2018.
- [31] Z. N. Mahmood, H. Al-Khazraji, and S. M. Mahdi, “PID-Based Enhanced Flower Pollination Algorithm Controller for Drilling Process in a Composite Material”, *Annales de Chimie Science des Matériaux*, Vol. 47, 2023.
- [32] A. M. Saeed, and K. S. Rijab, “PID controller enhanced A* algorithm for efficient water boat”, *J. Eur. Syst. Autom.*, Vol. 56, No. 6, pp. 1083-1093, 2023.
- [33] S. M. Mahdi, and S. M. Raafat, “Robust Interactive PID Controller Design for Medical Robot System”, *International Journal of Intelligent Engineering & Systems*, Vol. 15, No. 1, 2022, doi: 10.22266/ijies2022.0228.34.
- [34] L. T. Rasheed, N. Q. Yousif, and S. Al-Wais, “Performance of the optimal nonlinear PID controller for position control of antenna azimuth position system”, *Mathematical Modelling of Engineering Problems*, Vol. 10, No. 1, 2023.
- [35] H. Al-Khazraji, and L. T. Rasheed, “Performance evaluation of Pole Placement and Linear Quadratic Regulator strategies designed for Mass-Spring-Damper system based on Simulated Annealing and Ant Colony optimization”, *J. Eng.*, Vol. 27, No. 11, pp. 15-31, 2021.
- [36] Iswanto, N. M. Raharja, A. Ma’arif, Y. Ramadhan, and P. A. Rosyady, “Pole placement based state feedback for DC motor position control”, *J. Phys. Conf. Ser.*, Vol. 1783, p. 012057, 2021.
- [37] T. R. Farshi, “Battle royale optimization algorithm”, *Neural Computing and Applications*, Vol. 33, No. 4, pp. 1139-1157, 2021.
- [38] P. Trojovský, and M. Dehghani, “A new optimization algorithm based on mimicking the voting process for leader selection”, *PeerJ Comput. Sci.*, Vol. 8, No. e976, p. e976, 2022.
- [39] E. Trojovská, M. Dehghani, and V. Leiva, “Drawer algorithm: A new metaheuristic approach for solving optimization problems in engineering”, *Biomimetics (Basel)*, Vol. 8, No. 2, 2023.
- [40] P. D. Kusuma, and A. Dinimaharawati, “Swarm Bipolar Algorithm: A Metaheuristic Based on Polarization of Two Equal Size Sub Swarms”, *International Journal of Intelligent Engineering & Systems*, Vol. 17, No. 2, 2024, doi: 10.22266/ijies2024.0430.31.
- [41] A. Bhuvaneshwari, R. Hemalatha, and T. Satyasavithri, “Statistical tuning of the best suited prediction model for measurements made in Hyderabad city of Southern India”, In: *Proc of The World Congress on Engineering and Computer Science*, Vol. 2, 2013.
- [42] A. H. Tahoun, “Anti-windup adaptive PID control design for a class of uncertain chaotic systems with input saturation”, *ISA Trans.*, Vol. 66, pp. 176-184, 2017.